Pergamon

PII: S0042-6989(96)00015-6

Vision Res., Vol. 36, No. 18, pp. 2883–2896, 1996

Printed in Great Britain
0042-6989/96 $15.00 + 0.00

Psychophysical End-stopping Associated with Line Targets

CONG YU,*‡ EDWARD A. ESSOCK*†

Received 1 March 1995; in revised form 8 November 1995

Increment threshold for a small (e.g. 1′ × 5′) line target superimposed on backgrounds of various shapes and sizes was measured to provide a detailed map of the spatial interactions about line targets. This modified "Westheimer paradigm" indicated sensitization in the length direction as well as in the width direction around the line target. The effect of the adaptation field summed over an elongated, end-tapered central region, and showed strong end-zone antagonism beyond the ends of the elongated summation area, as well as flank antagonism to the sides. Secondary disinhibitory and inhibitory areas outside of the antagonistic surround were also demonstrated. When length of the test line was varied, the length of the summation region increased concomitantly, while the length of the end-zones remained fixed. End-zone antagonism was slightly weaker at oblique orientations. These results demonstrate a perceptual analog to neurophysiological end-stopping, and suggest a multilobed *y*-dimension weighting profile appropriate for models of spatial visual abilities. Copyright © 1996 Elsevier Science Ltd.

End-stopping Perceptive field Sensitization Adaptation

Although it has been 30 years since end-stopped receptive fields were first reported (Hubel & Wiesel, 1965, 1968), little information is available concerning the perceptual correlates of this receptive field property. Relatively recently several authors have proposed that end-stopped units play a central role in important perceptual abilities, such as: the detection of curved segments, corners, and line terminators in the visual image; the determination of foreground from background in regions of object occlusions; the reporting of illusory contours; and the accomplishment of low-level image segmentation (von der Heydt *et al.*, 1984; Dobbins *et al.*, 1987; von der Heydt & Peterhans, 1989; Versavel *et al.*, 1990; Heitger *et al.*, 1992; Wilson & Richards, 1992). Although originally viewed (Hubel & Wiesel, 1965, 1968) as a defining characteristic of a third class of cells beyond simple and complex cells (i.e. hypercomplex cells), end-stopping has been found in a majority of simple and complex cells and thus is now typically viewed as an additional dimension along which both simple and complex cells vary (Dreher, 1972; Schiller *et al.*, 1976; Gilbert, 1977; Henry, 1977; Murphy & Sillito, 1987; DeAngelis *et al.*, 1994). End-stopping is associated with inhibitory regions beyond the ends of the elongated receptive field center and is often termed "end-zone inhibition" (e.g. Bolz & Gilbert, 1986).

In the present research we investigate whether regions beyond the ends of a target line on a psychophysical task display antagonism similar to end-stopping in receptive fields. Specifically, we have adapted a paradigm popularized by Westheimer (1965, 1967) for measuring regions of spatial interactions around a test target. Westheimer and others noted that the effect of light near a small spot-shaped target suggested a local area of summation surrounded by an area of antagonism, much like center/surround receptive field antagonism (Westheimer, 1965, 1967; Fiorentini & Maffei, 1968; Enoch & Sunga, 1969; Oehler, 1985; Spillmann *et al.*, 1987). These regions of perceptual spatial interactions have subsequently been called "perceptive fields" to emphasize their similarity to receptive field shape (Jung & Spillmann, 1970). Indeed, when tested directly, single cells have been shown to display responses comparable to the human response on an equivalent test paradigm (Essock *et al.*, 1985). Responses of both humans and single cat cells are "desensitized" by near-by light and subsequently "sensitized" by light just outside of this central area (see also Shapley & Enroth-Cugell, 1984; Essock *et al.*, 1985; Cleland & Freeman, 1988; Hayhoe, 1990).

In the standard psychophysical paradigm, the increment threshold for a small spot (e.g. 1′) superimposed on

*Department of Psychology, University of Louisville, Louisville, KY 40292, U.S.A.

†Department of Ophthalmology and Visual Science, University of Louisville, Louisville, KY 40292, U.S.A.

‡To whom all correspondence should be addressed at present address: College of Optometry, University of Houston, Houston, TX 77204, U.S.A. [*Email* yucong@bayou.uh.edu].

a circular background of light is measured as a function of the diameter of the background field. As background diameter is increased, test threshold increases to a peak value, then decreases until a plateau is reached. This pattern of desensitization followed by sensitization has often been interpreted in terms of spatially antagonistic mechanisms affecting adaptation field effectiveness and (assuming Weber's law behavior) thereby driving threshold for this test probe first up, then down, as adaptation field size is increased (Shapley & Enroth-Cugell, 1984; Cleland & Freeman, 1988). For foveal photopic conditions, this paradigm routinely shows spatial interactions reflecting a 5–6′ diameter summation area surrounded by a concentric antagonistic area extending to *ca* 12–15′ diameter (e.g. Westheimer, 1967). In addition, at least one report suggests a weak disinhibitory area beyond this (D'Amico *et al.*, 1992).

A variation of this paradigm has been used to map perceptive fields about an elongated target (Fuld, 1978; Essock & Krebs, 1992; Essock *et al.*, 1997). Fuld (1978) measured the increment threshold of a small flickering line superimposed on a rectangular background whose length or width was varied. Sensitization was demonstrated that was consistent with elongated perceptive fields. Subsequently, full desensitization–sensitization curves in the width direction were demonstrated (Essock & Krebs, 1992) and obtained for static as well as flickered test lines. Because the perceptive field appears to be elongated (Fuld, 1978) and because the orientation anisotropy ("oblique effect") is observed (Essock & Krebs, 1992), these spatial interactions suggest a cortical locus, or a "cortical perceptive field" (see also Westheimer & Hauske, 1975; Williams *et al.*, 1983; Levi *et al.*, 1985; Williams & Essock, 1986). Furthermore, a subsequent report (Yu & Essock, 1996; Yu *et al.*, 1995) provides further evidence of a cortical locus based on the very steep spatial scaling functions (i.e. low E_2 values) demonstrated for the perceptive field antagonistic regions that are indicative of cortical processing. Although these elongated perceptive fields are known to be about 6′ wide with 3–4′ antagonistic flanks on either side, nothing is yet known about the length dimension or of the end-zone regions.

The goal of the present research was to systematically investigate spatial antagonism in the length dimension on a perceptual task. The length dimension has largely been ignored in models of pattern detection (e.g. Wilson & Gelb, 1984), as well as in the literature on spatial interactions revealed with adaptation fields. Little is known about the perceptual consequences of end-zone inhibition, its magnitude or spatial properties. In the present research, psychophysical end-stopping is investigated with adapting fields of various spatial configurations in a variation of the Westheimer paradigm. We demonstrate the existence of antagonistic end-zones in human target detection, map the size, strength, and orientation properties of the perceptual end-stopping, demonstrate that multiple antagonistic regions exist, and report that the spatial interactions closely match cortical end-stopping as well as recent reports of complexities of detailed cortical receptive field structure (Sun & Bonds, 1994). Brief reports of results in this paper were presented earlier (Yu & Essock, 1993; Yu *et al.*, 1994).

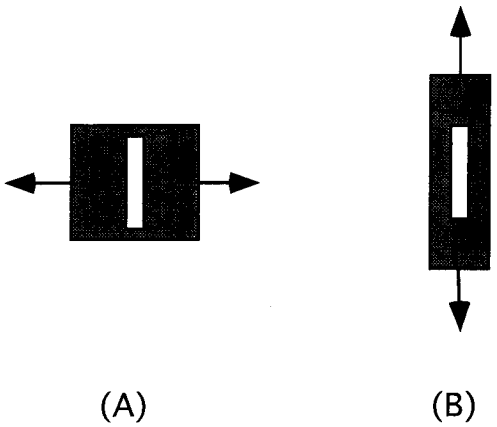

FIGURE 1. Stimulus configuration used in most experiments. A 1′-wide test line was centered on a rectangular background whose width (A) or length (B) was varied across conditions while the other dimension was held constant.

GENERAL METHODS

Observers

Between three and seven observers served in each experiment (eight female and five male in total, aged 20–35 yr). All subjects were emmetropic or wore an appropriate lens before the viewing eye to correct their vision to 20/20 or better. Only observers YC and JP had prior psychophysical experience. All were naive as to the purpose of the experiments except YC.

Apparatus and stimuli

The stimuli were generated by a Vision Works computer graphics system (Vision Research Graphics, Inc.) and presented on a Nanao Flexscan 9080i color monitor. Pixel size was 0.17′ horizontal × 0.25′ vertical, 1024 × 512 resolution, and the frame rate was 117 Hz. Brightness of the monitor was linearized by means of an 8-bit look-up table for each gun. Subjects were positioned 5.64 m from the screen by means of a chin rest. Viewing was monocular (dominant eye) with a white translucent diffuser positioned before the other eye.

In all experiments an increment test field (Field I) and a background field (Field II) were presented on the center of the 2.8 deg × 2.1 deg monitor screen (Field III). The test field was a small line (1′ × 5′ in most experiments) centered on a rectangular background as depicted in Fig. 1. In most experiments either the length or the width of the background field was fixed and the other dimension was varied. In other experiments, the rectangular background was fixed and combined with additional shapes whose configuration was varied. The sides of the rectangular backgrounds were parallel to the sides of

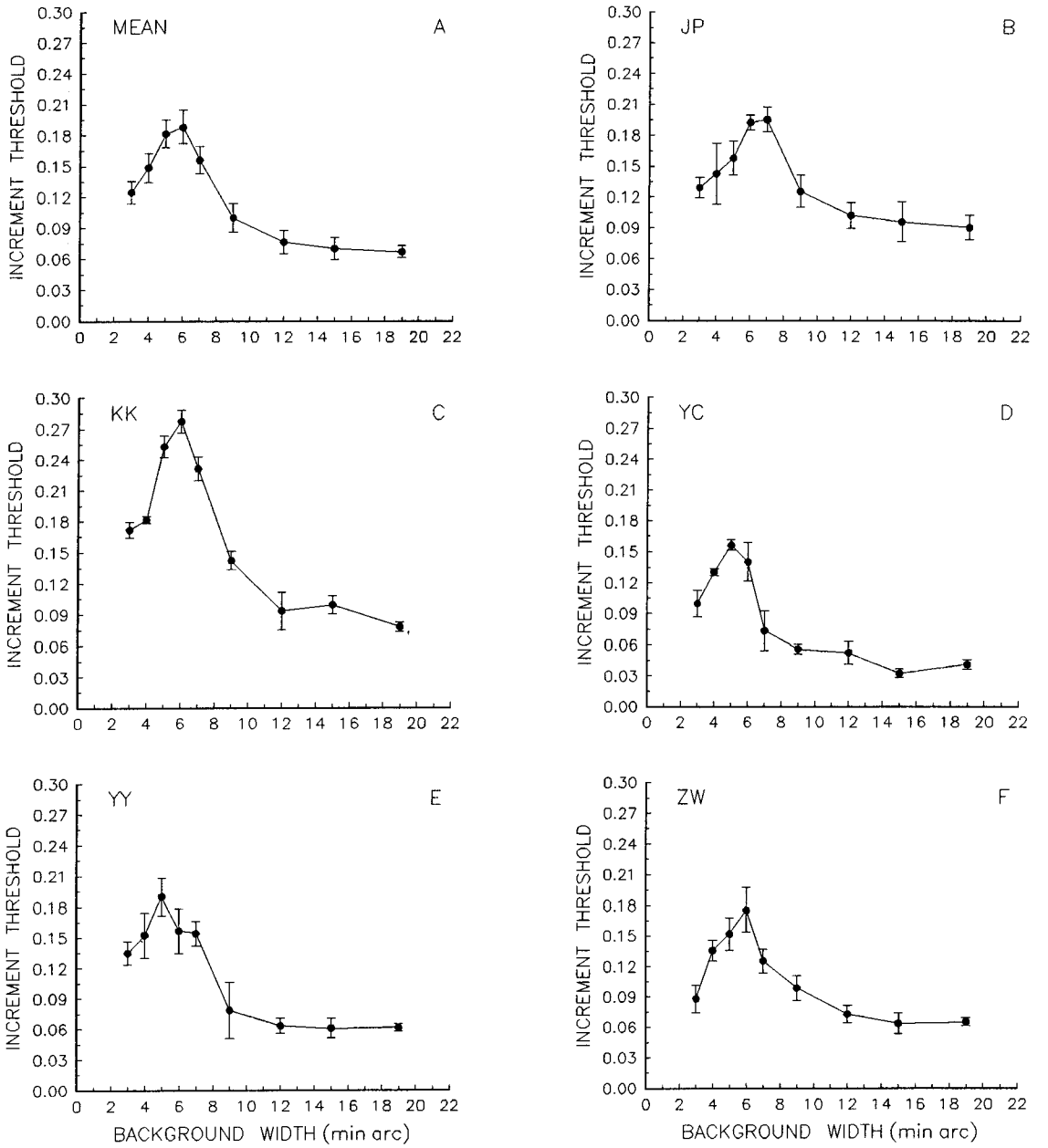

FIGURE 2. Width summation and flank antagonism at 0 deg (vertical) target orientation. Increment threshold is plotted as a function of background width with background length fixed at 6′. In this and all later figures, increment threshold is plotted as $\log(I + \Delta I) - \log I$ and error bars represent ± 1 SEM, and error bars plotted for group means indicate the average of the subjects' standard errors.

the test line in all experiments. The luminance of the screen and background field were 6.8 and 47.7 cd/m^2, respectively, and the luminance of the test line was varied by a staircase procedure.

Procedure

A successive two-alternative forced-choice (2AFC) procedure was used. The background field was present in each of the two intervals (680 msec) and during the interstimulus interval (340 msec). In one of the two intervals the test line was also presented. The screen luminance always remained constant both throughout and between trials. Each trial was preceded by a 6.3′ × 6.3′ fixation cross in the center of the screen which disappeared 100 msec before the beginning of the trial. Intervals were marked by tones, and another tone provided feedback on incorrect responses.

Each staircase consisted of four "practice" reversals and six experimental reversals. Each correct response lowered test field luminance by one step and each correct response raised test luminance by three steps. Step size was 0.6 cd/m^2 in the experimental phase and 3.6 cd/m^2 at the beginning of the practice phase with step size decreasing to 1.8 cd/m^2 by the end of the practice phase.

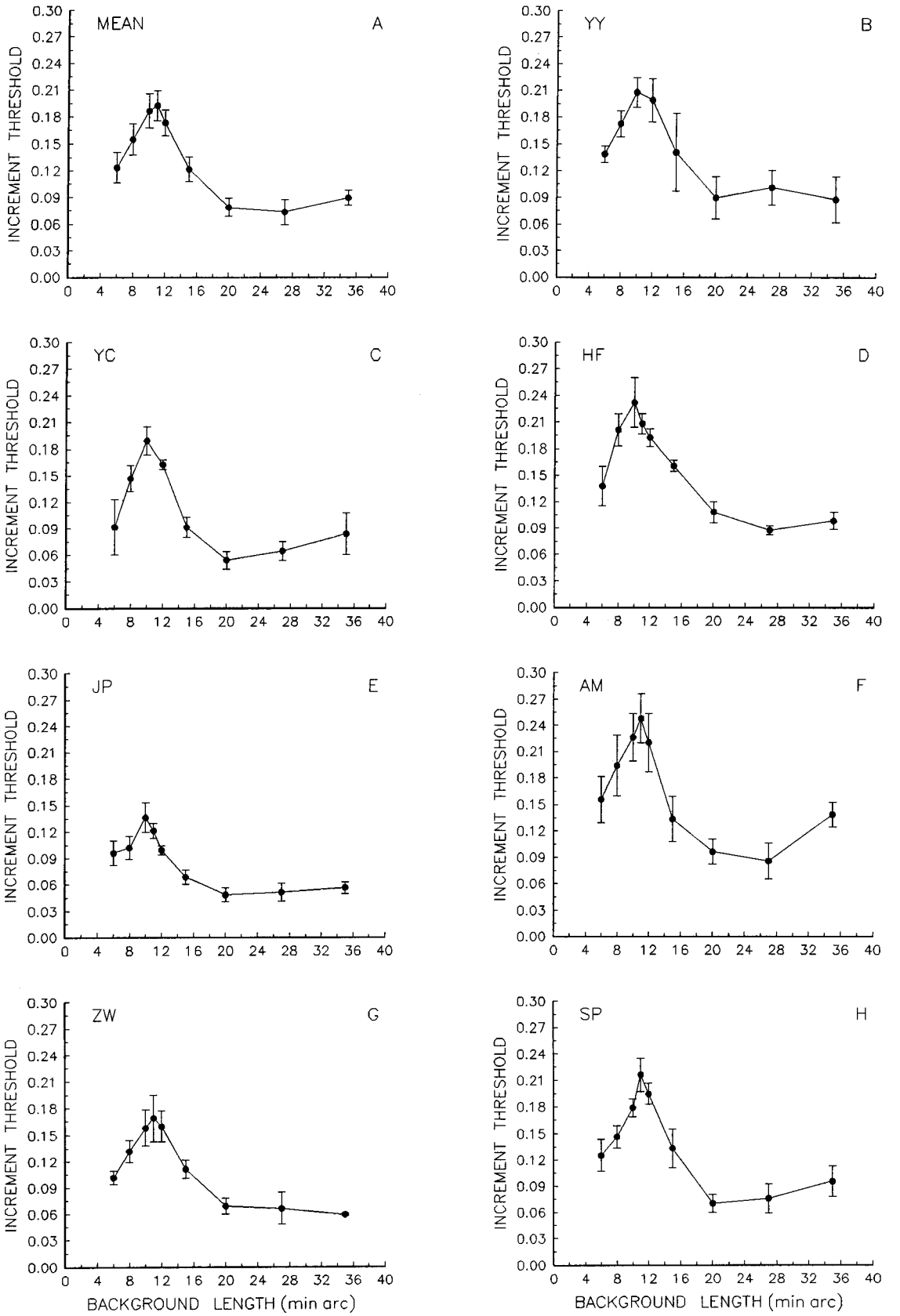

FIGURE 3. Length summation and end-zone antagonism at 0 deg target orientation. Increment threshold is plotted as a function of background length with background width fixed at 3′.

The mean of six experimental reversals was used to estimate the increment threshold which was defined as the difference of log target luminance at threshold and log background luminance ($\log(\Delta L + L) - \log L$).

An experimental session consisted of eight to ten staircases, typically one for each background size of the experiment, and lasted approximately 50 min. All conditions were tested in random order within each session. Each data point represents the mean of four to six replications for each condition, and the error bars represent ± 1 SEM.

EXPERIMENT 1: SPATIAL INTERACTIONS ABOUT A LINE TARGET

The effect of steady background light located to the sides of a test line was first measured as a baseline condition. In order to minimize any end-zone effects, the rectangular background was set to 6′, just 1′ longer than the $1' \times 5'$ test line. Background width was varied between 3′ and 19′. Average thresholds and average standard errors are shown in Fig. 2(A) for the five subjects tested.

At the smaller backgrounds (3′ through 6′), the effect of the background appears to approximate Ricco's Law with threshold elevation approximately proportional to background area. Peak threshold is reached at a width of 5′ or 6′ depending on the subject. At larger background widths, threshold decreases first rapidly then much more slowly as an asymptote is approached, with the bulk of the threshold decline reached by a width of 12′. Thus, summation occurs within a 5′–6′-wide region and light outside of this central area has an antagonistic effect, lowering thresholds until a width of *c.* 14′ is reached. This pattern of desensitization, sensitization, and plateau is comparable to that shown by Westheimer (1967) for a circular target and circular background. The data replicate the findings reported by Essock and Krebs (1992) for similar test conditions. The spatial interactions were quite consistent across observers [Fig. 2(B)–(F)], with each observer showing a central summation area of 5′ or 6′ width and inhibitory flanks *c.* 3.5′–4.5′ wide each.

We next varied the length of the background in order to measure summation along the long axis of the line target and to reveal any end-zone antagonism beyond this region. In order to avoid the lateral inhibitory flanking regions demonstrated in Fig. 2, we fixed the width of the background to 3′, a width well inside the 5–6′-wide center region. Seven observers were tested at nine background lengths, 6′, 8′, 10′, 11′, 12′, 15′, 20′, 27′, and 35′ (except the first two subjects, YC and YY, who were not tested at the 11′ length). Mean data presented in Fig. 3(A) show both very clear summation and very pronounced outlying antagonism along the long axis of the test line. Again all subjects [Fig. 3(B)–(H)] are quite consistent, showing summation until a length of 10′ (four subjects) or 11′ (three subjects) and antagonism until *c.* 23′. As in the width direction, threshold approaches asymptote very slowly with antagonism extending to about 23′ on average, with the bulk of the antagonism occurring by a width of 18′–20′. Comparison of the extent of summation in the length direction (Fig. 3) to the extent of summation in the width direction (Fig. 2) indicates that the central summation area is considerably elongated, about twice as long as it is wide ($5.5' \times 10.5'$ on average). Beyond the ends of the elongated center are 5′–6′ long inhibitory end-zone areas assuming symmetry.* Thus, these results demonstrate strong antagonism beyond the ends of a line target on a perceptual detection task. The end-zone inhibition of these elongated perceptive fields suggests a strong similarity to the receptive field property of end-stopping seen in many single cortical cells. In addition, about half of the subjects also show evidence of further threshold elevation beyond the end-zone region at a background length of about 35′. Similar disinhibition has been reported around a circular target in the Westheimer paradigm (D'Amico *et al.*, 1992).

The present data clearly delimit the length and width of the summation region, flanks, and end-zones, and thereby clarify some of the puzzling aspects of Fuld's (1978) prior study. Foremost is that his failure to obtain full desensitization–sensitization functions appears to be due in part to the limited range of background sizes employed, as he suggested. Fuld's smallest foveal background size should have been just big enough to reveal peaks in his variable-length condition, and just too small to reveal desensitization in his variable-width condition. Although Fuld was unable to show the desensitization branch and thus unable to provide clear evidence of peaks, we show that his conclusion that the center region is elongated was correct and that his estimate of the total perceptive field area (0.08 deg^2) was quite close to ours although he had assumed a circular antagonistic surround. The present results show that the total lateral extent of the perceptive field is about 13.5′ and the length of the total perceptive field is about 21.5′, yielding a total area of about 0.06–0.08 deg^2 (based on the shape of the "corners" detailed below).

EXPERIMENT 2: LENGTH ANTAGONISM AT DIFFERENT TARGET ORIENTATIONS

If the elongated summation areas and associated antagonistic areas reflect cortical processes related to the detection of elongated targets, then they should show certain changes as the orientation of the test or background configuration is changed. First, although he was unable to measure the sizes of these regions, work by Fuld (1978) was suggestive of perceptive fields elongated in the direction of the long axis of a line, whether horizontal or vertical. Secondly, Essock and Krebs (1992) demonstrated that the flanking inhibition produced by a bright static background was much stronger

*Electrophysiological reports indicate that end-stopping is typically present at both end-zones, but often asymmetrical in strength (Orban *et al.*, 1979a, b; Yamane *et al.*, 1985) or length (Peterhans & von der Heydt, 1993). Since perceptive fields are likely to reflect the composite properties of a number of similar units detecting the target, we will assume symmetry when inferring perceptive field size from desensitization–sensitization curves.

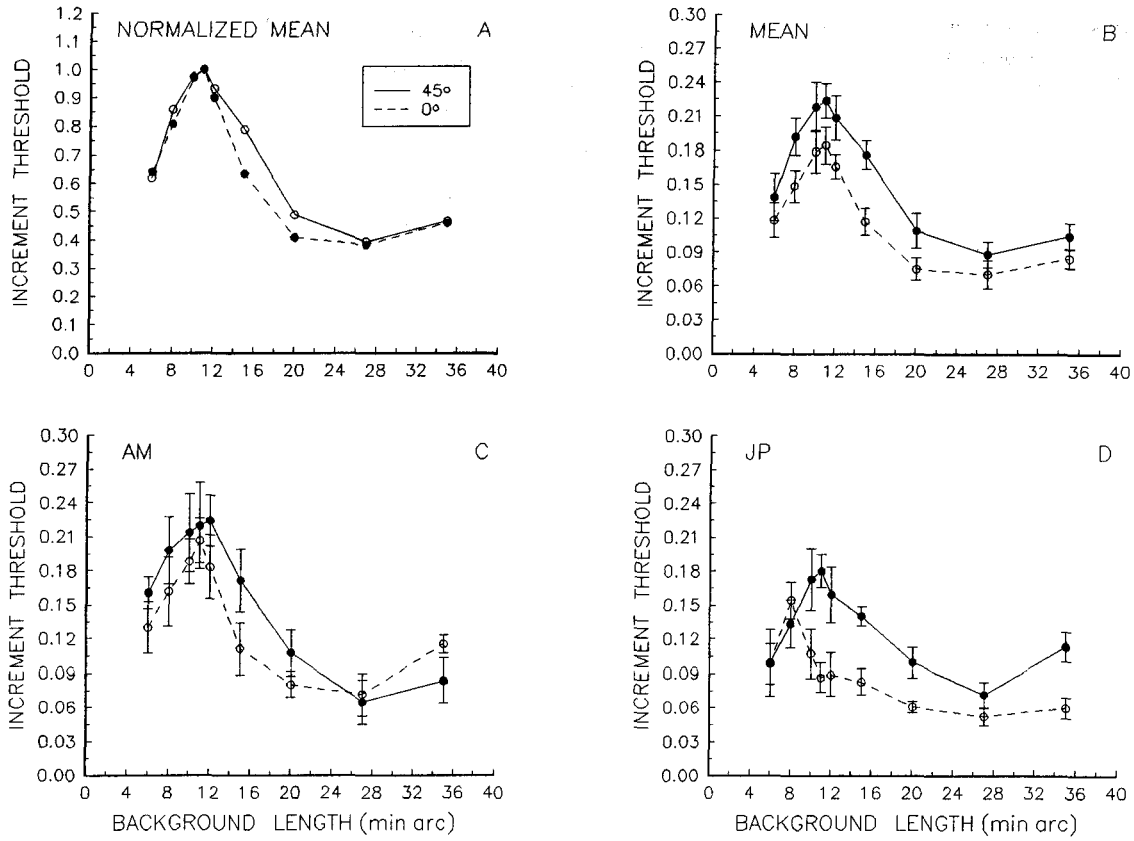

FIGURE 4. Length summation and end-zone antagonism at 45 deg clockwise (solid line) and 0 deg (dotted line) target orientations. Normalized mean (A), mean (B) and individual data from two of five observers (C and D) are shown.

for horizontal or vertical (H–V) test orientations than for oblique test line orientations. This weaker oblique flanking inhibition is consistent with examples of greater visual responses for H–V targets and also with greater intra-channel orientation inhibition at H–V orientations (Essock & Krebs, 1992). Both of these findings suggest a cortical locus for these line-target perceptive fields.

In this experiment we wanted to determine whether there was an oblique bias of perceptual end-zone inhibition comparable to the orientation bias of flanking inhibition. We tested five observers at both 0 and 45 deg orientations of the test/background configuration. Indeed, when tested at oblique orientations, the subjects showed a small but consistent orientation bias. The curves were normalized to their peak value so that their shapes could be directly compared [Fig. 4(A)]. The end-zone antagonism associated with oblique orientations was slightly weaker (i.e. slower sensitization as background size is increased). This effect is similar to but smaller than the weaker flank inhibition demonstrated previously with this

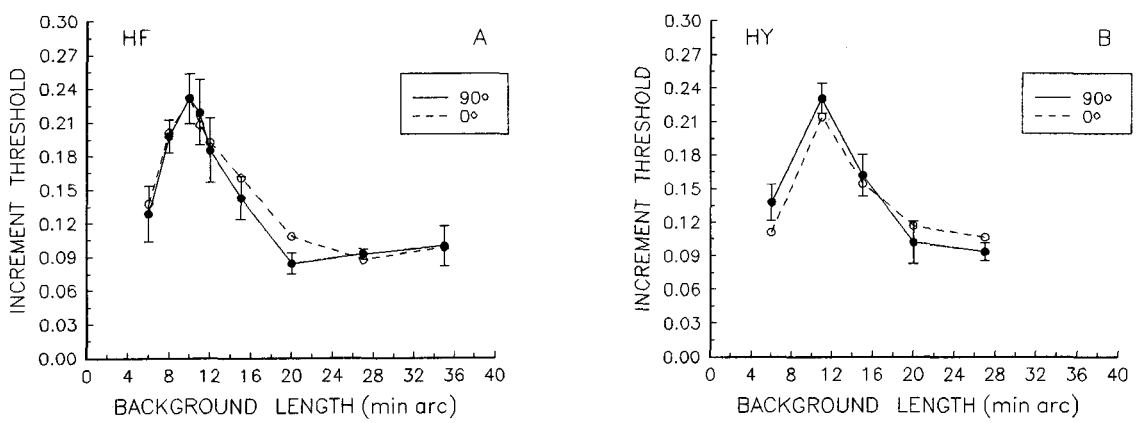

FIGURE 5. Length summation and end-zone antagonism at 90 deg, horizontal, (solid line) and 0 deg, vertical, (dotted line) orientations from two observers.

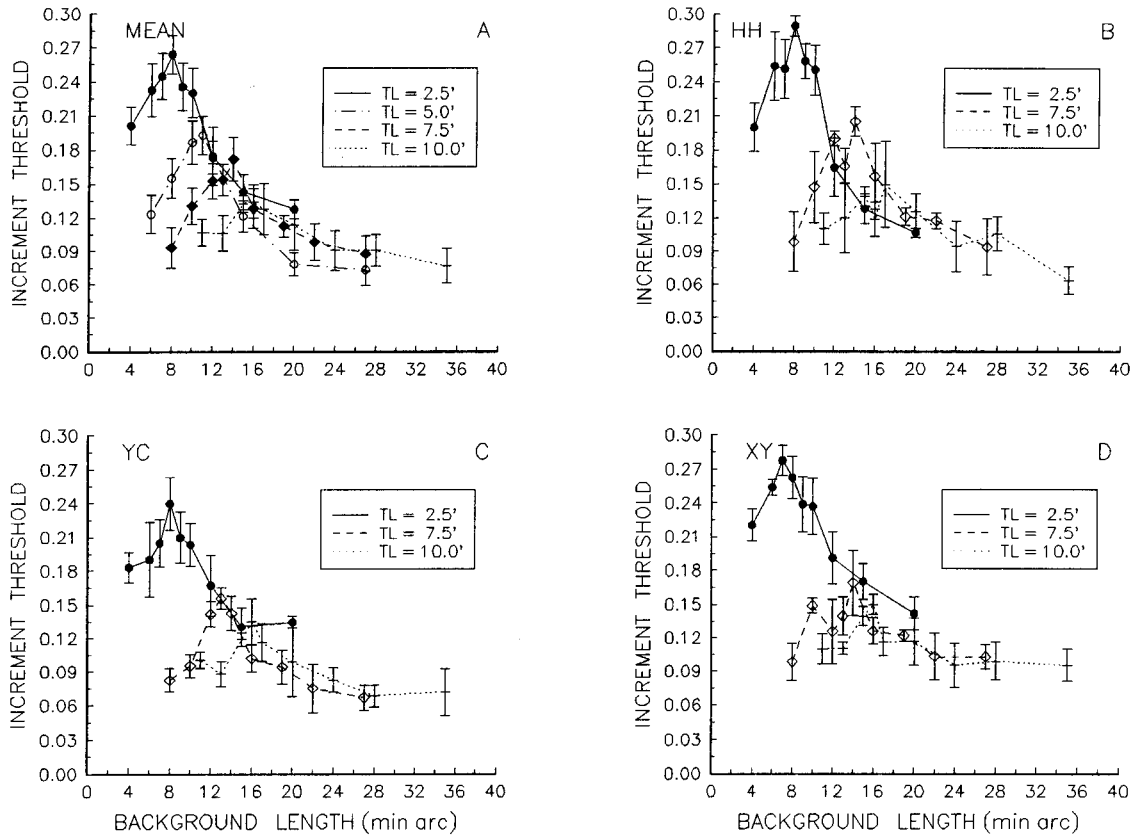

FIGURE 6. Length summation and end-zone antagonism at different test line lengths. Mean data and data with the 5′ line length [replotted from Fig. 3(A)] are shown in (A). (B)–(D) Individual data. (TL = Test-line length).

paradigm (Essock & Krebs, 1992). The end-zone anisotropy reported in the present study appears to be a smaller effect than the flank anisotropy, but since the magnitude of the oblique effect is known to vary across individuals, comparison across the different observers of the two studies is difficult. In addition to this sensitization anisotropy, oblique line thresholds are generally higher, consistent with the well-established sensitivity anisotropy (e.g. Rentschler & Fiorentini, 1974). The overall threshold difference is seen in Fig. 4(B) where the raw data are plotted. Individual data for two of the five subjects are shown in Fig. 4(C) and (D). This anisotropy is truly a bias of obliques since a comparison of 0 and 90 deg orientations showed no difference between these orientations [Fig. 5(A) and (B)].

EXPERIMENT 3: END-STOPPING FOR TARGETS OF DIFFERENT LENGTHS

This experiment investigated whether a different extent of the end-zone regions and length of the summation area was associated with target lines of different lengths. Three observers (HH, XY, and YC) were tested with 1′ wide target lines that were either 2.5, 7.5, or 10′ in length. Threshold was measured as a function of the length of a 3′ wide background. Average thresholds are shown in Fig. 6(A) for 2.5, 7.5, and 10′ lines along with the average data for a 5′ line replotted from Fig. 3 which were obtained under comparable conditions but with different subjects. The four curves show a very regular progression as the length of the test line is increased. The curves in general show regular desensitization–sensitization branches, although the magnitude of desensitization and sensitization is weaker for longer test lines. The peak threshold shifted to a larger background size as line length is increased (8, 11, 14, and 16′ for target lengths of 2.5, 5.0, 7.5, and 10.0′, respectively), indicating that larger summation areas are associated with longer test lines. As is typical for perceptive fields, the exact extent of the antagonistic regions is more difficult to determine as the sensitization branches of the curves reach their plateau very gradually. Fitting a smooth curve by eye suggests that the curves level off at *c.* 21, 23, 29, and 30′ for the 2.5, 5.0, 7.5, and 10.0′ test lines, respectively. Thus, the shorter the length of the test lines, the shorter and stronger are the summation and antagonistic regions associated with them.

The increase in length of the summation area with increased test line length corresponds quite closely to the amount by which the length of the test line was increased in each case. That is, the length of the summation area is directly attributable to the length of the test line. The extent of the central summation zone is 6′ greater than the length of the test line regardless of line length

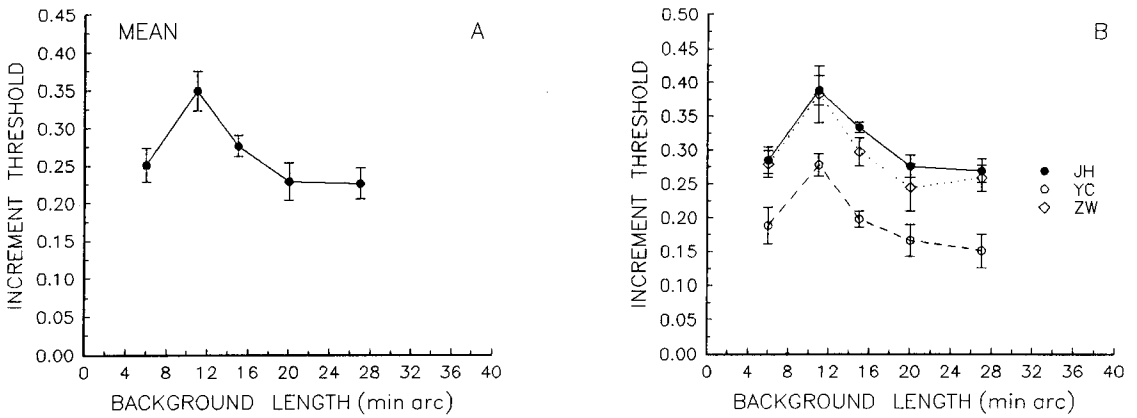

FIGURE 7. (A) Length summation and end-zone antagonism measured for a target consisting of only the ends of a test line. (B) Individual data.

[specifically, 5.5, 6.0, 6.5, and 6.0′ greater than the test line length for lengths of 2.5, 5.0, 7.5, and 10.0′, respectively, on the mean curves shown in Fig. 6(A)]. The slope of the regression of summation region length on test line length is *c.* 1.0 (summation length = 1.08 × test-line length + 5.50). Assuming that this region is centered on the test, this suggests that the summation area extends *c.* 3′ beyond either end of the test line regardless of line length. Although difficult to delineate as precisely, the length of the end-zone antagonism appears to be constant, roughly 6–7′ long on either end (on average, end-zone length = 0.06 × test-line length + 6.25). Thus, the length of the center region scales with test line length, but the length of the end-zone regions do not. Over this range of line lengths, the perceptive fields can be thought of as consisting of a central summation region extending about 3′ beyond each end of the test line, regardless of length of line, and an antagonistic end-zone region extending *c.* 6.5′ beyond each end of the central region. For these test conditions, the extent of the spatial interactions is clearly greater in the length dimension than in the width dimension. The antagonistic regions extend about 6–7′ in length, but the flanks appear to extend only about 3.5–4.5′ to either side (Fig. 2).

The findings that the summation area extends a constant distance beyond either end of the test line regardless of line length and that length of the end-zones is independent of test line length suggest that the ends of the test line may be the critical feature rather than the area or flux of the line. In other words, the middle part of the test line may play little or no role in determining the length of the summation area and in eliciting the end-stopping. This was tested by presenting three subjects with only the ends of a test line presented on a set of five background lengths (3′ wide). The increment stimulus consisted of two 1′ × 1′ squares separated by a 3′ vertical gap (that is, a 1′ × 5′ test line with the central 1′ × 3′ area removed). Results (Fig. 7) clearly show spatial interactions comparable to those for a full 1′ × 5′ line target; peak desensitization occurs at the 11′ background size and sensitization levels off in the neighborhood of the 20′ background. These results are consistent with the common suggestion in the literature that line stimulus can be defined functionally either psychophysically or neurophysiologically by the endpoints of the line

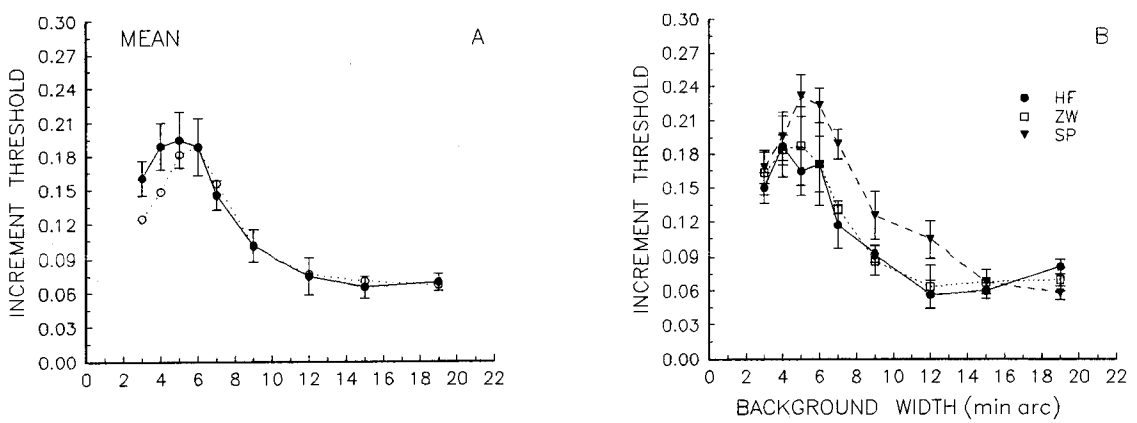

FIGURE 8. Width summation and flank antagonism measured with background whose length (11′) covered the summation area. (A) Mean data and data obtained with a 6′-long background (dashed line) replotted from Fig. 2(A). (B) Individual data.

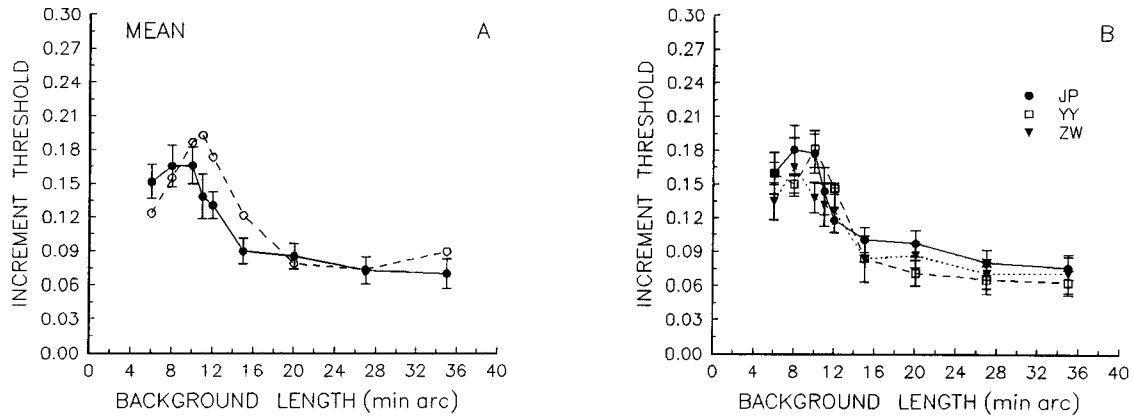

FIGURE 9. Length summation and end-zone antagonism measured with the background width equal to the full width of the summation center (5′ or 6′ for different observers, see text). (A) Mean data for a 5–6′-wide background (solid line) and mean data for a 3′-wide background (dotted line) replotted from Fig. 3(A). (B) Individual data.

(Sullivan *et al.*, 1972; Swindale & Cynader, 1989). It is also noteworthy that similar effects have been reported for a two-dot target with a task of alignment (vernier acuity) rather than increment threshold (Williams & Essock, 1986).

EXPERIMENT 4: BOUNDARY BETWEEN THE SUMMATION AND INHIBITION REGIONS

Together the length and width conditions of Experiment 1 demonstrated that the central summation area is elongated. Specifically, the sensitivity profile in the length direction associated with a $1' \times 5'$ target line was measured for the central 3′ portion of the 5–6′-wide summation region, and in the width direction for the central 6′-portion of the 10–11′ long summation region. In order to gain more information about the corners of the $5–6' \times 10–11'$ central summation area (areas not in the most central 3′-wide, 6′-long portion of this region), the spatial interactions for a background whose size just covered the full length of the center (11′) and the full width of the center (5 or 6′) was employed.

Three subjects (HF, SP, and ZW) were tested with the background length fixed at 11′ to cover the full length of the summation area, while the background width was varied in nine steps between 3′ and 19′. These results are shown in Fig. 8(A) (mean data, solid line) and Fig. 8(B) (individual data). Fig. 8(A) also replots the mean data for the 6′-long background condition [from Fig. 2(A), obtained with different observers] for comparison [dashed line in Fig. 8(A)]. Although similar curves are seen for both background length conditions, the threshold elevation across the smaller background widths is much more gradual for the current 11′-long background condition. The slower accumulation of desensitization as the background is widened for the 11′-long background condition suggests that the strength of summation is less in the ends of the elongated center area relative to the central 6′-long region, implying narrower or weaker summation regions. The greater level of threshold elevation at smaller background widths for the 11′-long background condition is attributable to the larger background covering more of the total summation area. Specifically, this difference seen comparing the 3′ point on the 11′-length curve ($3' \times 11'$) and the 3′ point on the 6′-length curve ($3' \times 6'$) is the same phenomenon as that seen in Fig. 3 for a 3′ fixed-width background as the length is increased and fills more of the center. The more important comparison is the steepness, rather than the level, of the desensitization, which is what suggests that the size or strength of the summation region is quite nonuniform across the ends of the $6' \times 11'$ area.

These outer "corners" of the summation area were investigated in an analogous way for a series of backgrounds that were varied in length, rather than width. This time the background width was set to match the extent of the center area and length was varied so that these results could be compared to the prior results from varying length when the width of the background filled only the central 3′ of the center region (Fig. 3). The background width in this experiment was chosen individually for each observer to match the background width at which each person previously showed peak threshold (5′ for YY and 6′ for JP and ZW, see Fig. 2). These results are shown in Fig. 9. In order to compare the curve shapes for the variable-length data for the central portion of the summation area (the 3′-wide data, Fig. 3) and the present variable-length results obtained over the full width of the summation area, the 3′-wide data are replotted in Fig. 9(A) along with the mean of the full-width data. When the full width of the center is covered, desensitization (summation) is much weaker, with both a smaller total magnitude and shallower slope as compared to when the background covers only the central 3′-wide portion of the $5–6' \times 10–11'$ central area (Fig. 9). Furthermore, the peaks in two of three observers' curves (JP and ZW) shift to a smaller background [Fig. 3(E) vs solid curve in Fig. 9(B), Fig. 3(G) vs dotted curve in Fig. 9(B)], suggesting that the desensitization seen with a 3′-

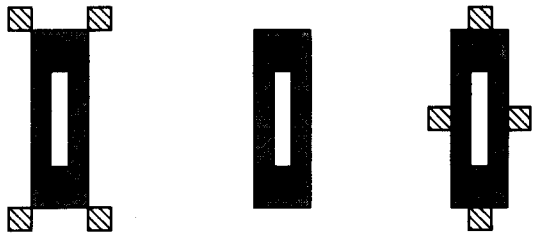

FIGURE 10. Stimulus configurations for measuring the shape of the summation center. (A) $3' \times 9'$ rectangle with four $1' \times 1'$ squares located by its corners; (B) rectangle only; (C) $3' \times 9'$ rectangle with $1' \times 1'$ squares abutting the midpoints of its sides.

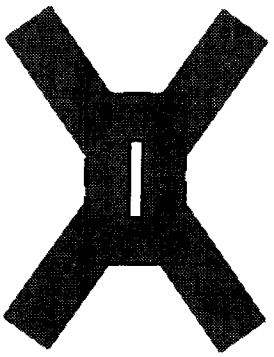

FIGURE 12. Stimulus used to measure the outer-limits of the surround. It consisted of a $6' \times 11'$ rectangle (highlighted by dotted lines which are themselves not presented in the stimulus) and two 3'-wide bars of the same intensity oriented ± 35 deg. The rectangle was fixed and the length of the bars was varied.

wide background may be counteracted by an antagonistic influence in the corners of the $5–6' \times 10–11'$ center region. Thus, the results of both the variable-width series [Fig. 8(A)] and this variable-length series [Fig. 9(A)] suggest that the central summation area is tapered on the ends (i.e. like a rectangle with the corners cut off).

Whether the central summation region is tapered, specifically, whether the "corners" of the central $5–6' \times 10–11'$ region are indeed inhibitory, was tested directly by comparing threshold for different shapes of background field. The background consisted of a rectangle set to $3' \times 9'$, thereby covering only the central portion of the summation region, and four adjacent $1' \times 1'$ squares added to it. The squares were set to 122.3 cd/m^2 to emphasize the effects of these very small areas and the rectangle remained at 47.7 cd/m^2. In one condition the squares were placed at the corners of this rectangle ('A' in Fig. 10), in a second condition they were absent ('B' in Fig. 10), and in a third condition they were placed in the middle of the four sides of the rectangle ('C' in Fig. 10). Figure 11 shows the effect of background configuration on threshold ($F(2,6) = 20.05$, $P < 0.01$). Relative to the control condition (squares absent), the presence of dots at the "corner" areas causes sensitization, and placement of the same squares in the middle of the background's four sides results in additional desensitization. These results provide strong evidence that the central summation area is 10–11' long only in the middle region (i.e. the middle 3' of width) and is 6' wide only across the middle portion (i.e. the middle 6' of length). That is, the summation area is tapered on the ends with antagonistic regions outside of the tapered center at these "corners".

EXPERIMENT 5: OUTER LIMITS OF THE SURROUND REGION

The experiments reported above indicate that the total width of the flank inhibition is about 14' and that the end-zone inhibition extends to about 23' for a $1' \times 5'$ target line. The nature of the region in between the antagonistic end-zones and flanks is not yet clear. Since the summation area was found to be tapered, a tapered inhibitory area, with flank inhibition blending into end-zone inhibition might be expected. To measure the extent of the inhibition outside of the tapered center's "corners", and to determine whether inhibition exists

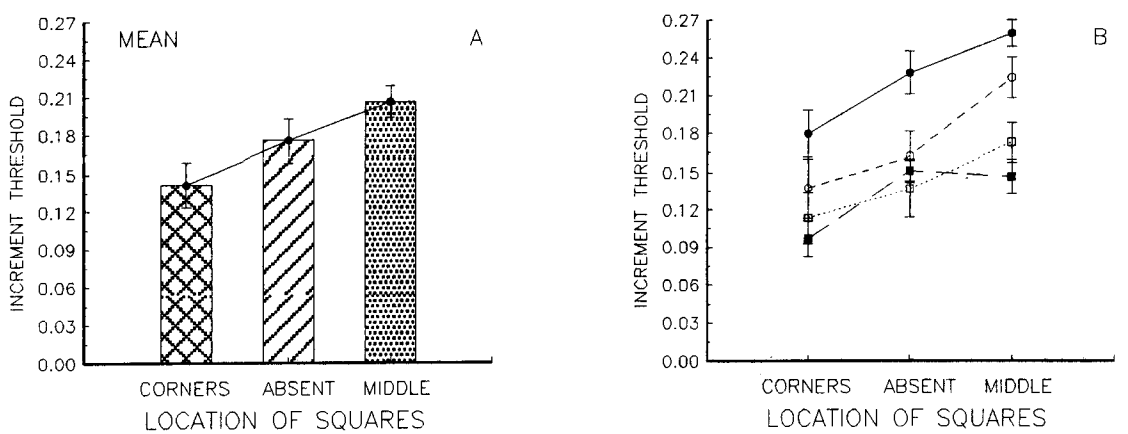

FIGURE 11. Increment threshold obtained for the three stimulus configurations shown in Fig. 10.

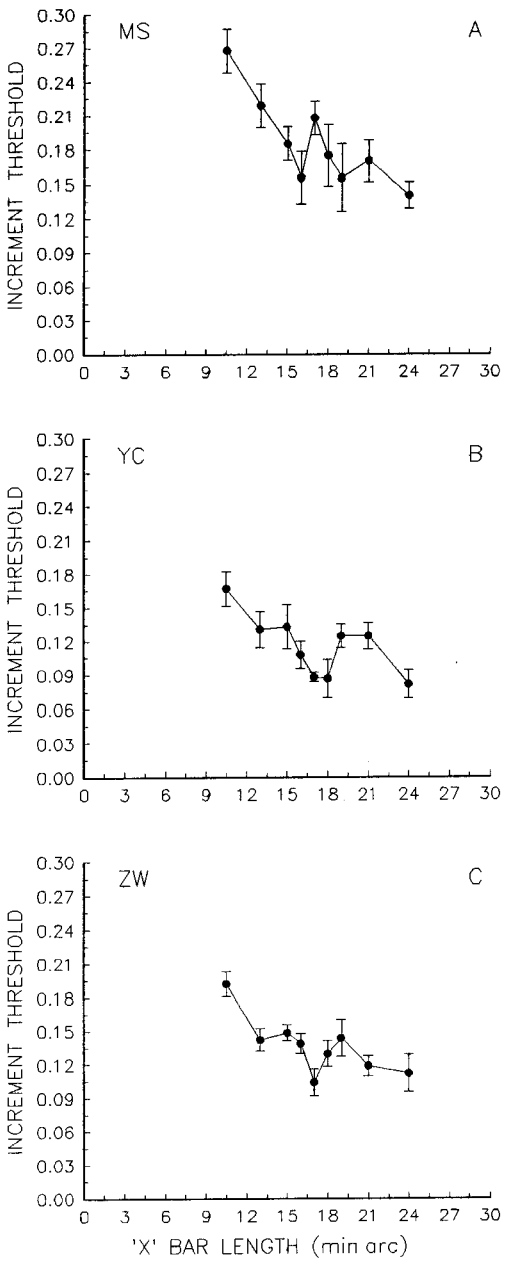

FIGURE 13. Increment threshold as a function of the length of the X-shaped bars shown in Fig. 12.

between the inhibitory flanks and the end-zones, we next employed a background shape that emphasized these regions. The background (Fig. 12) consisted of an 'X'-shape of two crossed bars (± 35 deg from the vertical axis) superimposed upon a $6' \times 11'$ rectangular background (both 47.7 cd/m^2). The $6' \times 11'$ rectangle fully covered the central summation area and the bars of the 'X' were extended across the corner regions where the prior experiments suggested inhibitory spatial interactions. The bars of the 'X' were varied in length from 10.5′, a value not extending outside of the central background rectangle, to 24′, the full extent of the possible inhibitory region (a $14' \times 20'$ rectangle).

The results (Fig. 13) show a general trend of decreased

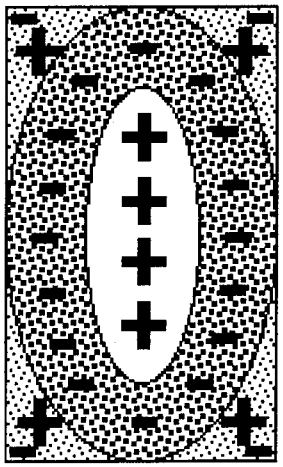

FIGURE 14. A two-dimensional map of the spatial interactions obtained in this study. The perceptive field is formed with a tapered excitatory center, a tapered inhibitory surround consisting of a confluence of end-zone antagonism and flank antagonism, and secondary outlying excitatory and inhibitory areas.

threshold suggesting that the regions outside of an end-tapered central summation area continue to be inhibitory. Surprisingly, however, all three subjects tested show an interruption in the general pattern of threshold decline by a sharp threshold elevation at middle X-bar lengths. Thresholds for all three observers decline to bar lengths of 16–18′, suggesting an inhibitory region, then show a very abrupt elevation suggesting an excitatory (or disinhibitory) area that is only about 2′ wide, followed by renewed inhibition. The prior results show that the inhibitory flanks extend to about 14′ laterally and the inhibitory end-zones extend to about 23′ in the length direction, while the present results indicate that at an angle of ± 35 deg the initial inhibitory area extends to about 17′. Thus, together these results suggest an elliptical, or tapered, surround region, around a tapered center region. Outside of this surround at ± 35 deg the X-bar experiment indicates a very narrow region of strong disinhibition with additional inhibitory areas outside of that. These disinhibitory regions could be related to prior reports of flank disinhibition (Rentschler & Hilz, 1976; Wilson *et al.*, 1979; Wilson, 1986). An alternative account of the effect of the X-bar background is to consider it as an oriented masking stimulus, producing cross-channel inhibition [or gain alteration, Gaska *et al.* (1994), Geisler & Albrecht (1992), and Wilson & Humanski (1993)] on the vertically oriented detecting mechanism. Although reports of orientation masking on increment threshold tasks exist (Waugh *et al.*, 1993), such an effect does not fit well with the observed effects (specifically a localized increase in increment threshold over a highly localized region corresponding only to medium-size bar lengths between 16–18′ length).

The general configuration of these spatial interactions is shown in Fig. 14. It represents a perceptive field with a tapered excitatory center, a tapered inhibitory surround

consisting of a confluence of end-zone antagonism and flank antagonism, and secondary outlying excitatory and inhibitory areas. There are no clear borders between the flanks and end-zones. In general, this configuration resembles a typical end-stopped simple cell receptive field.

GENERAL DISCUSSION

The present results delineate the spatial interactions revealed by an adapting field in a line-detection task. Compared to the effects of adaptation fields on small circular targets (e.g. Westheimer, 1965, 1967), these spatial interactions are relatively complex. We have demonstrated that light within a central elongated, end-tapered, 5–6′ × 10–11′ region elevates threshold of a 1′ × 5′ line target (desensitization), that light outside of this central region lowers threshold (sensitization) over an end-tapered 14′ × 23′ region, and that light beyond the "corners" of this outer tapered region (i.e. at ±35 deg from vertical) has a disinhibitory effect (desensitization) over a very narrow area, then a further inhibitory effect outside of this region (Fig. 14). Most importantly, the present results provide a psychophysical demonstration and delineation of antagonism beyond the ends of the test line in the "end-zone" regions.

Viewed in terms of a psychophysical analog to receptive fields, these results suggest "perceptive fields" (Jung & Spillmann, 1970) that are elongated with strong end-zone antagonism in addition to flank antagonism. These fields appear to reflect cortical-level spatial processes because: (1) they are highly elongated and oriented in nature; (2) they show an "oblique effect" orientation bias (Fuld, 1978; Essock & Krebs, 1992; Fig. 5); and (3) the elongated perceptive fields observed with a line target are not observed for a circular target on a rectangular background (Fuld, 1978). Moreover, when the end-zone and flank antagonism was measured at the different eccentricities (Yu & Essock, 1996; Yu *et al.*, 1995), their dramatically steeper spatial scaling functions, or lower E_2 values, as compared with those of line detection with no adapting background ($E_2 = 0.45$ for end-zone antagonism, 0.77 for flank antagonism, and 2.05 for line detection) undoubtedly point to a cortical explanation. Perceptive fields are likely to reflect the composite spatial profile of the handful of cells that are the most sensitive to the test pattern and hence mediating detection at threshold (Teller, 1980; Jung & Spillmann, 1970). Thus the map shown in Fig. 14 may reflect the composite profile of the units detecting a small (1′ × 5′) foveal test line. The size of the end-zone antagonism observed psychophysically in the present study fits with the smaller of the end-stopped primate receptive fields (Peterhans & von der Heydt, 1993). The width of the elongated perceptive fields observed here corresponds closely to the 5–6′ width of foveal perceptive fields obtained for circular targets (Westheimer, 1967; Spillmann *et al.*, 1987) which very closely match the center size of M-cell receptive fields (Oehler, 1985), the retinal cell type with the highest contrast sensitivity (see Crook *et al.*, 1988).

When line-length was varied in the present study, it was observed that the end-zone region *per se*, remained constant and the length of the center region increased in a way that matched the increase of the length of the target line. These results are consistent with a model in which these cortical perceptive fields are formed by the combination of the appropriate number of circular perceptive fields, whose centers overlie the target line (cf. Hubel & Wiesel, 1962). This would produce a constant length of end-zone regions, a fixed length of summation observed beyond the endpoints of the test line, and a total length of summation that matches the line length plus a constant (the fixed amount beyond the endpoints). The results are also similar to the finding that various end-stopped cells are length-tuned (show summation) to different stimulus lengths (Sillito, 1977; Peterhans & von der Heydt, 1993). Additional intracortical mechanisms, however, are likely to impart the bulk of end-zone inhibition. For example, Bolz and Gilbert (1986) have disassociated end-zone and flank inhibition by pharmacological means by demonstrating abolishment of end-inhibition while flank properties were preserved. The slightly different spatial scale observed here for perceptive field flank (3.5–4.5′) and end-zone inhibition (6–7′) is consistent with such a distinction.

Multiple antagonistic lobes or disinhibitory regions have been reported in both psychophysical and electrophysiological studies. D'Amico *et al.* (1992) observed disinhibition on this paradigm with a circular stimulus. Disinhibitory lateral and length-direction spatial interactions have been demonstrated in cat receptive fields (Li *et al.*, 1992; Li & Li, 1994), and multi-lobed receptive fields have been shown in cat and monkey (Movshon *et al.*, 1978; De Valois *et al.*, 1978). In the present study, evidence of secondary excitatory and inhibitory areas was obtained at outlying regions located ±35 deg from vertical (Fig. 13). Similar effects were not seen when the background dimension was varied either parallel or perpendicular to the target line orientation (Experiment 1). Although the background width or length steps used in Experiment 1 were not as fine as in the 'X' bar experiment, especially in length experiment, we measured one subject (ZW) with very fine steps (1–2′) in the length direction, and the threshold after the sensitization branch was basically unchanged, suggesting no secondary spatial interactions beyond the end-zone. The combination of additional areas of excitation at ±35 deg and the elongated central excitatory region results in a spatial profile that is very similar to a type of cat cortical receptive fields reported recently by Sun and Bonds (1994). These authors used a sensitive reverse correlation technique to map detailed receptive field structure and found numerous secondary excitatory and inhibitory regions across the receptive field. One type of receptive field structure that they reported [e.g. their Figure 4(A)] resembles a 'Y'-shape where an elongated central region is linked with additional excitatory regions

in the "corners" similar to our results from the X-bar experiment showing additional excitatory and inhibitory areas at ± 35 deg. A composite of such 'Y'-shaped excitatory regions and inverted 'Y'-shapes is strikingly similar to the perceptive fields mapped in the present study.

Numerous models of spatial vision are based on low-level filters which resemble simple-cell receptive fields (e.g. Nielsen *et al.*, 1985; Carlson & Klopfenstein, 1985; Klein & Levi, 1985; Wilson & Gelb, 1984; Waugh *et al.*, 1993). These models often use mechanisms with the *x*-dimension sensitivity profiles specified by a difference-of-Gaussians (DOG), or similar function consisting of a central area with one or more antagonistic flanks. The models account very well for many basic features of visual performance such as detection performance, spatial and orientation tuning and associated aftereffects. Typically the length dimension has been ignored in spatial vision models (e.g. Kulikowski & King-Smith, 1973; Wilson, 1978), but some reports have modeled it as a *y*-dimension Gaussian (Kulikowski *et al.*, 1973; Bacon & King-Smith, 1977; Phillips & Wilson, 1984; Wilson, 1986; Parker & Hawken, 1988). Specifically, the length to width ratio found here for the center region compares favorably with the ratios of the *x*- and *y*-dimension Gaussians in models of spatial vision (Phillips & Wilson, 1984) and to ratios of V1 simple and complex cells (Parker & Hawken, 1988). The present results involving the spatial interactions of local light adaptation indicate that end-zone inhibition plays a fairly early role in visual detection and suggest that a consideration of antagonism in the *y*-direction must be considered at some level in such models. In particular, the present results suggest that when models of spatial vision are extended to describe performance on tasks involving more complex two-dimensional visual patterns, or tasks involving curvature, terminators, occlusions, and related image cues, incorporation of significant end-zone antagonism and possibly secondary spatial interaction regions as well will be required. The interactions sketched in Fig. 14 indicate that a *y*-axis weighting function that is itself multilobed, such as a DOG with a greater spatial scale than in the *x*-direction, might be more appropriate than a simple single-lobed weighting function.

REFERENCES

Bacon, J. & King-Smith, P. E. (1977). The detection of line segments. *Perception, 6*, 125–131.

Bolz, J. & Gilbert, C. D. (1986). Generation of end-inhibition in the visual cortex via interlaminar connections. *Nature, 320*, 362–365.

Carlson, C. R. & Klopfenstein, R. W. (1985). Spatial-frequency model for hyperacuity. *Journal of the Optical Society of America A, 2*, 1747–1751.

Cleland, B. G. & Freeman, A. W. (1988). Visual adaptation is highly localized in the cat's retina. *Journal of Physiology, 404*, 591–611.

Crook, J. M., Lange-Malecki, B., Lee, B. B. & Valberg, A. (1988). Visual resolution of macaque retinal ganglion cells. *Journal of Physiology, 396*, 205–224.

D'Amico, J., Yager, D. & Bichao, C. (1992). Oscillations in Westheimer functions: Psychophysical evidence for multiple excitatory and inhibitory regions. *Investigative Ophthalmology and Visual Science (Suppl.), 33*, 3257.

DeAngelis, G. C., Freeman, R. D. & Ohzawa, I. (1994). Length and width tuning of neurons in the cat's primary visual cortex. *Journal of Neurophysiology, 71*, 347–374.

De Valois, R. L., Albrecht, D. G. & Thorell, L. G. (1978). Cortical cells: Bar and edge detectors, or spatial frequency filters? In Spekreijse, H. & van der Tweel, H. (Eds), *Spatial contrast* (pp. 60–63). Amsterdam: Elsevier.

Dobbins, A., Zucker, S. W. & Cynader, M. S. (1987). Endstopped neurons in the visual cortex as a substrate for calculating curvature. *Nature, 329*, 438–441.

Dreher, B. (1972). Hypercomplex cells in the cat's striate cortex. *Investigative Ophthalmology, 11*, 355–356.

Enoch, J. & Sunga, R. (1969). Development of quantitative perimetric tests. *Documental Ophthalmology, 26*, 215–229.

Essock, E. A. & Krebs, W. K. (1992). Sensitization of a line target depends on orientation and temporal modulation. *Investigative Ophthalmology and Visual Science (Suppl.), 33*, 1349.

Essock, E. A., McCarley, J. S., Sinai, M. J., Khang, B. G., Lehmkuhle, S., Krebs, W. K. & Yu, C. (1997). Extensions of the sustained-like and transient-like effects. In: V. Lakshminarayanan (Ed.), *Basic and clinical applications of Vision Science*. Dordrecht, Netherlands: Kluwer Academic Press.

Essock, E. A., Lehmkuhle, S., Frascella, J. & Enoch, J. M. (1985). Temporal modulation of the background affects the sensitization response of X- and Y-cells in the dLGN of cat. *Vision Research, 25*, 1007–1019.

Fiorentini, A. & Maffei, L. (1968). Perceptual correlates of inhibitory and facilitatory spatial interactions in the visual system. *Vision Research, 8*, 1195–1203.

Fuld, K. (1978). A sensitization effect with rectangular stimulus. *Vision Research, 18*, 1045–1051.

Gaska, J. P., Jacobson, L. D., Chen, H. & Pollen, D. A. (1994). Space–time spectra of complex cell filters in the macaque monkey: A comparison of results obtained with pseudowhite noise and grating stimuli. *Visual Neuroscience, 11*, 805–821.

Geisler, W. S. & Albrecht, D. G. (1992). Cortical neurons: Isolation of contrast gain control. *Vision Research, 32*, 1409–1410.

Gilbert, C. D. (1977). Laminar differences in receptive field properties of cells in cat primary visual cortex. *Journal of Physiology, 268*, 391–421.

Hayhoe, M. M. (1990). Spatial interactions and models of adaptation. *Vision Research, 30*, 957–965.

Heitger, F., Rosenthaler, L., von der Heydt, R., Peterhans, E. & Kubler, O. (1992). Simulation of neural contour mechanisms: From simple to end-stopped cells. *Vision Research, 32*, 963–981.

Henry, G. H. (1977). Receptive field classes of cells in the striate cortex of the cat. *Brain Research, 133*, 1–28.

von der Heydt, R. & Peterhans, E. (1989). Mechanisms of contour perception in monkey visual cortex. I. Lines of pattern discontinuity. *Journal of Neuroscience, 9*, 1731–1748.

von der Heydt, R., Peterhans, E. & Baumgartner, G. (1984). Illusory contours and cortical neuron responses. *Science, 224*, 1260–1262.

Hubel, D. H. & Wiesel, T. N. (1962). Receptive fields, binocular interaction and functional architecture in the cat's visual cortex. *Journal of Physiology, 160*, 106–154.

Hubel, D. H. & Wiesel, T. N. (1965). Receptive fields and functional architecture in two nonstriate visual areas (18 and 19) of the cat. *Journal of Neurophysiology, 28*, 229–289.

Hubel, D. H. & Wiesel, T. N. (1968). Receptive fields and functional architecture of monkey striate cortex. *Journal of Physiology, 195*, 215–243.

Jung, R. & Spillmann, L. (1970). Receptive-field estimation and perceptive integration in human vision. In Young, F. A. & Lindslay D. B. (Eds), *Early experience and visual information processing in perceptual and reading disorders* (pp. 181–197). Washington DC: National Academy of Sciences.

Klein, S. A. & Levi, D. M. (1985). Hyperacuity thresholds of 1 sec: Theoretical predictions and empirical validation. *Journal of the Optical Society of America A, 2*, 1170–1190.

Kulikowski, J. J., Abadi, R. & King-Smith, P. E. (1973). Orientational selectivity of grating and line detectors in human vision. *Vision Research, 13*, 1479–1486.

Kulikowski, J. J. & King-Smith, P. E. (1973). Spatial arrangement of line, edge and grating detectors revealed by subthreshold summation. *Vision Research, 13*, 1455–1478.

Levi, D. M., Klein, S. A. & Aitsebaomo, A. P. (1985). Vernier acuity, crowding and cortical magnification. *Vision Research, 25*, 963–977.

Li, C. Y. & Li, W. (1994). Extensive integration field beyond the classical receptive field of cat's striate cortical neurons—classification and tuning properties. *Vision Research, 34*, 2337–2355.

Li, C. Y., Zhou, Y. X., Pei, X., Qiu, F. T., Tang, C. Q. & Xu, X. Z. (1992). Extensive disinhibitory region beyond the classical receptive field of cat retinal ganglion cells. *Vision Research, 32*, 219–228.

Movshon, J. A., Thompson, I. D. & Tolhurst, D. J. (1978). Spatial summation in the receptive fields of simple cells in the cat's striate cortex. *Journal of Physiology, 283*, 53–77.

Murphy, P. C. & Sillito, A. M. (1987). Corticofugal feedback influences the generation of length tuning in the visual pathway. *Nature, 329*, 727–729.

Nielsen, K. R., Watson, A. B. & Ahumada, A. J. (1985). Application of a computable model of human spatial vision to phase discrimination. *Journal of the Optical Society of America A, 2*, 1600–1606.

Oehler, R. (1985). Spatial interactions in the rhesus monkey retina: A behavioral study using the Westheimer paradigm. *Experimental Brain Research, 59*, 217–225.

Orban, G. A., Kato, H. & Bishop, P. O. (1979a). End-zone region in receptive fields of hypercomplex and other striate neurons in the cat. *Journal of Neurophysiology, 42*, 818–832.

Orban, G. A., Kato, H. & Bishop, P. O. (1979b). Dimensions and properties of end-zone inhibitory areas in receptive fields of hypercomplex cells in cat striate cortex. *Journal of Neurophysiology, 42*, 818–832.

Parker, A. J. & Hawken, M. J. (1988). Two-dimensional spatial structure of receptive fields in monkey striate cortex. *Journal of the Optical Society of America A, 5*, 598–605.

Peterhans, E. & von der Heydt, R. (1993). Functional organization of area V2 in the alert macaque. *European Journal of Neuroscience, 5*, 509–524.

Phillips, G. C. & Wilson, H. R. (1984). Orientation bandwidths of spatial mechanisms measured by masking. *Journal of the Optical Society of America A, 1*, 226–232.

Rentschler, I. & Fiorentini, A. (1974). Meridional anisotropy of psychophysical spatial interactions. *Vision Research, 14*, 1467–1473.

Rentschler, I. & Hilz, R. (1976). Evidence for disinhibition in line detectors. *Vision Research, 16*, 1299–1302.

Schiller, P. H., Finlay, B. L. & Volman, S. F. (1976). Quantitative studies of single-cell properties in monkey striate cortex. I. Spatiotemporal organization of receptive fields. *Journal of Neurophysiology, 39*, 1288–1319.

Shapley, R. & Enroth-Cugell, C. (1984). Visual adaptation and retinal gain controls. *Progress in Retinal Research, 3*, 263–343.

Sillito, A. M. (1977). The spatial extent of excitatory and inhibitory zones in the receptive field of superficial layer hypercomplex cells. *Journal of Physiology, 273*, 791–803.

Spillmann, L., Ransom-Hogg, A. & Oehler, R. (1987). A comparison of perceptive and receptive fields in man and monkey. *Human Neurobiology, 6*, 51–62.

Sullivan, G. D., Oatley, K. & Sutherland, N. S. (1972). Vernier acuity as affected by target length and separation. *Perception and Psychophysics, 12*, 438–444.

Sun, M. & Bonds, A. B. (1994). Two-dimensional receptive-field organization in striate cortical neurons of the cat. *Visual Neuroscience, 7*, 703–720.

Swindale, N. V. & Cynader, M. S. (1989). Vernier acuities of neurons in area 17 of cat visual cortex: Their relation to stimulus length and velocity, orientation selectivity, and receptive-field structure. *Visual Neuroscience, 2*, 165–176.

Teller, D. Y. (1980). Locus questions in visual science. In Harris, C. S. (Ed.), *Visual coding and adaptability* (pp. 69–94). Hillsdale, NJ: Lawrence Erlbaum Associates.

Versavel, M., Orban, G. A. & Lagae, L. (1990). Responses of visual cortical neurons to curved stimuli and chevrons. *Vision Research, 30*, 235–248.

Waugh, S. J., Levi, D. M. & Carney, T. (1993). Orientation, masking, and vernier acuity for line targets. *Vision Research, 33*, 1619–1638.

Westheimer, G. (1965). Spatial interaction in the human retina during scotopic vision. *Journal of Physiology, 181*, 812–894.

Westheimer, G. (1967). Spatial interaction in human cone vision. *Journal of Physiology, 190*, 139–154.

Westheimer, G. & Hauske, G. (1975). Temporal and spatial interference with vernier acuity. *Vision Research, 15*, 1137–1141.

Williams, R. A. & Essock, E. A. (1986). Areas of spatial interaction for a hyperacuity stimulus. *Vision Research, 26*, 349–360.

Williams, R. A., Essock, E. A. & Enoch, J. M. (1983). Influence of variable-sized backgrounds on a hyperacuity threshold. In Breinin, G. M. & Siegel, F. M. (Eds), *Advances in diagnostic visual science*. Heidelberg: Springer Series in Optical Sciences, 41, Springer.

Wilson, H. R. (1978). Quantitative characterization of two types of line-spread function near the fovea. *Vision Research, 18*, 971–981.

Wilson, H. R. (1986). Responses of spatial mechanisms can explain hyperacuity. *Vision Research, 26*, 453–469.

Wilson, H. R. & Gelb, D. J. (1984). Modified line element theory for spatial frequency and width discrimination. *Journal of the Optical Society of America A, 1*, 124–131.

Wilson, H. R. & Humanski, R. (1993). Spatial frequency adaptation and contrast gain control. *Vision Research, 33*, 1133–1149.

Wilson, H. R., Phillips, G., Rentschler, I. & Hilz, R. (1979). Spatial probability summation and disinhibition in psychophysically measured line-spread functions. *Vision Research, 19*, 593–598.

Wilson, H. R. & Richards, W. A. (1992). Curvature and separation discrimination at texture boundaries. *Journal of the Optical Society of America A, 9*, 1653–1662.

Yamane, S., Maske, R. & Bishop, P. O. (1985). Properties of end-zone inhibition of hypercomplex cells in cat striate cortex. *Experimental Brain Research, 60*, 200–203.

Yu, C. & Essock, E. A. (1993). Psychophysical end-zone inhibition demonstrated with the Westheimer paradigm. *Investigative Ophthalmology and Visual Science (Suppl.), 34*, 418.

Yu, C. & Essock, E. A. (1996). Spatial scaling of end-stopped perceptive fields: Differences in neural bases of end-zones, flanks, and centers. *Vision Research*, in press.

Yu, C., Khang, B., Sinai, M. J. & Essock, E. A. (1994). Two-dimensional properties of end-stopped perceptive fields associated with line detection. *Investigative Ophthalmology and Visual Science (Suppl.), 35*, 3472.

Yu, C., McCarley, J. S. & Essock, E. A. (1995). Psychophysical end-stopping, flank inhibition, and central summation of perceptive fields are based on different neural substrates. *Investigative Ophthalmology and Visual Science (Suppl.), 36*, 2146.

Acknowledgements—This research was supported by Fight-For-Sight Grant GA90095 and a Grant-in-Aid of Research from Sigma Xi.